SUPPLEMENTARY DATA

Table S1- A list of genes with differential expression in epidermis between K14cre-/SmoM2+ and K14cre+/SmoM2+ mice. These 595 genes were filtered as Significant from Student's t-test comparing the GL(SMO+/K14cre-) to GLSM(SMO+/K14cre+). Student's t-test was done on RMA + quantile summarized and absent filtered dataset, 165 probe set with equal means were also filtered out. The cut-off p-value is p <=0.05 with no adjustment (see attached).

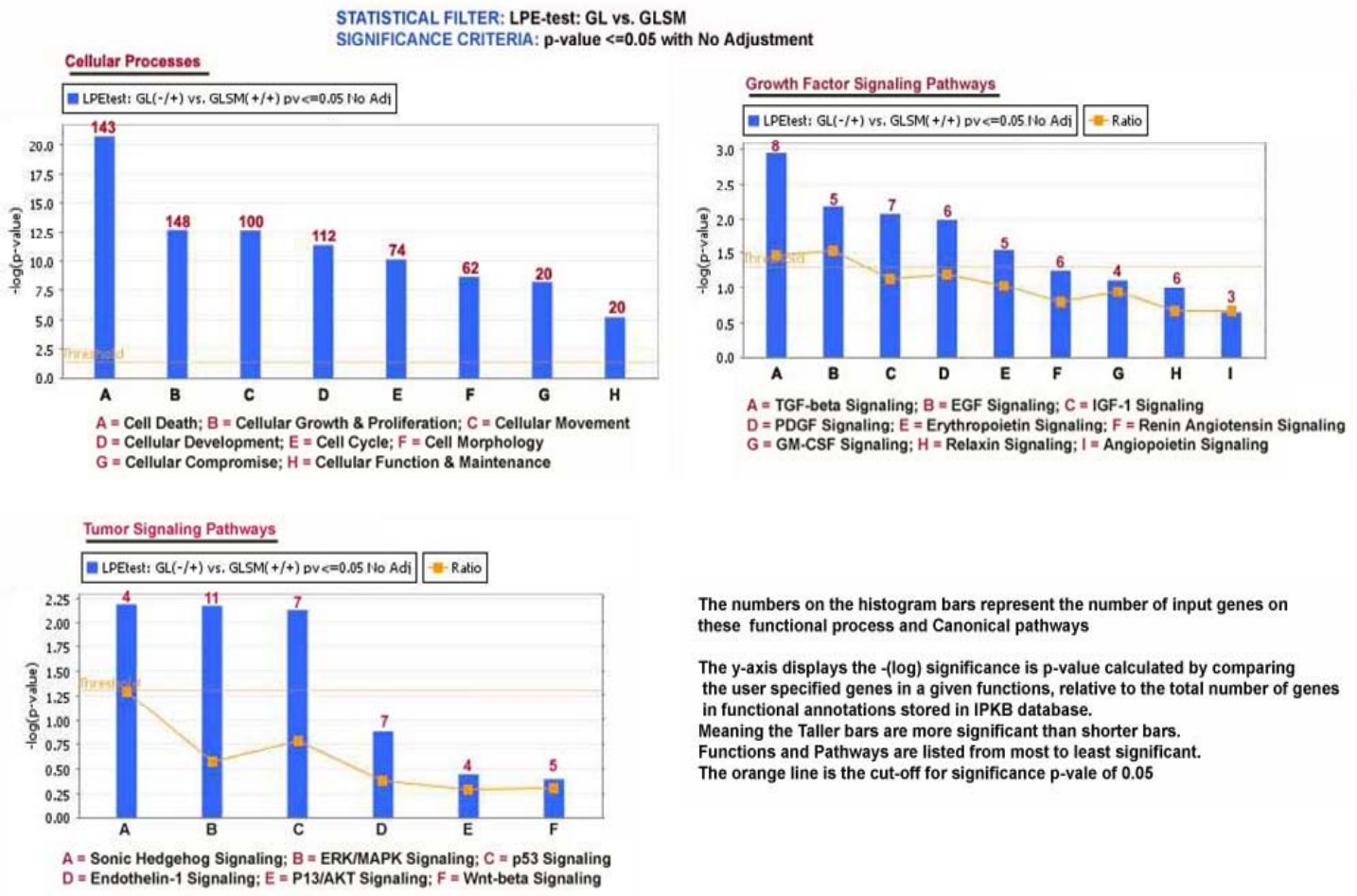

Fig. S1 Alteration of signaling pathways in epidermis with SmoM2 expression, derived from Ingenuity pathway analysis. Ingenuity pathway analysis was performed using the probe sets with p< 0.05. As expected, the Hh pathway was altered in this mouse model. Other major pathways altered in this mouse model include the TGFβ pathway, ERK/MAP signaling, EGF, IGF-1 and PDGF signaling pathways.

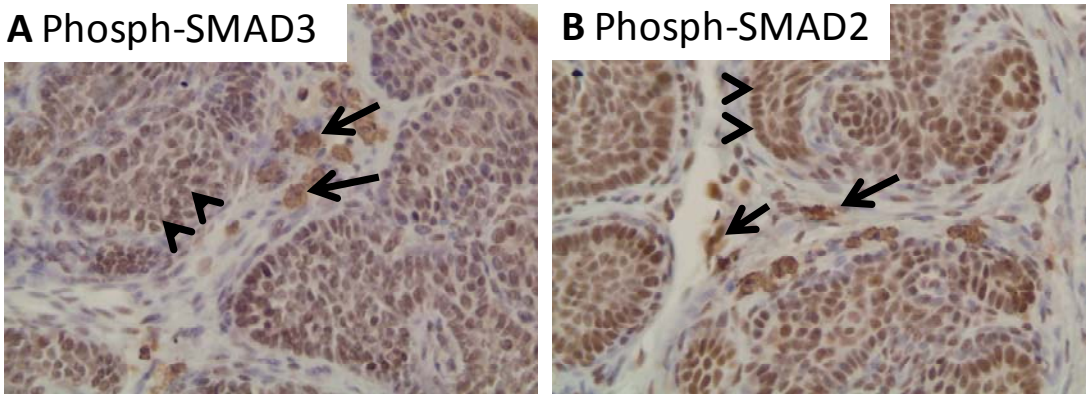

Fig. S2 Detection of phosphorylated SMAD2 and SMAD3 in SmoM2-mediated tumors. Immunohistochemistry was performed using a standard avidin-biotin immunostaining kit from Vector Laboratories Inc and specific antibodies to phospho-SMAD2 (**A**, antibodies from Cell Signaling Inc., dilution of 1:200), phosph-SMAD3 (**B**, antibodies from Santa Cruz Biotechnology Inc., dilution of 1:200). Positive staining is brown (indicated by arrows in the tumor and arrow bars in the stroma). Hematoxylin was used for counter staining (blue in the nucleus).

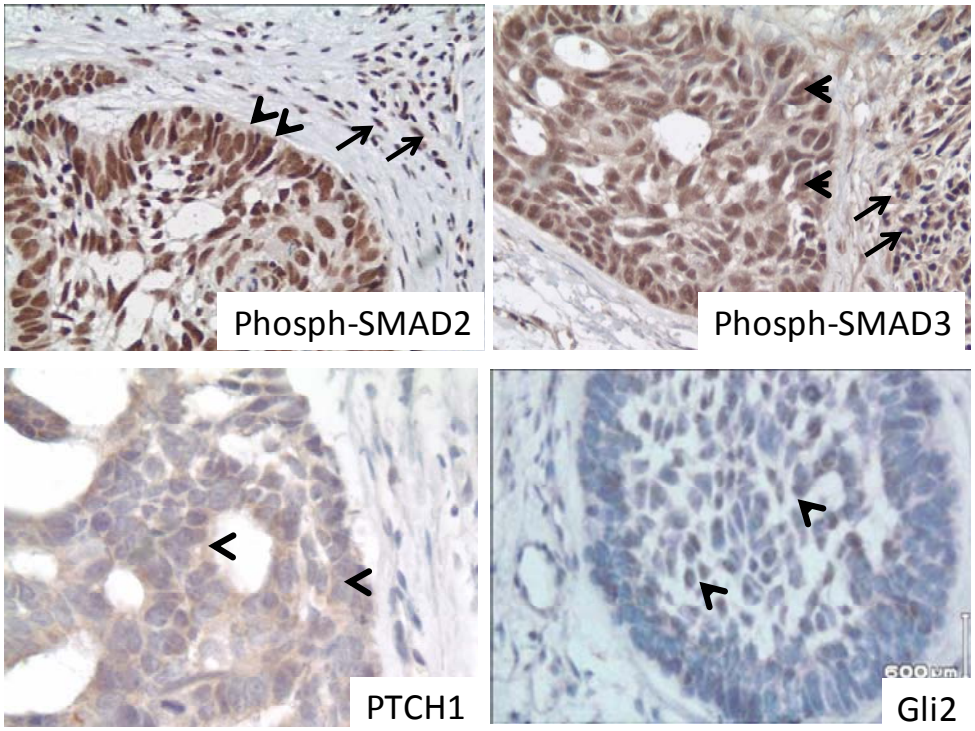

Fig. S3 Detection of phosphorylated SMAD2 and Gli2 in human BCCs. Immunohistochemistry was performed using a standard avidin-biotin immunostaining using a kit from Vector laboratories and specific antibodies to phospho-SMAD2 (Cell Signaling Inc., dilution of 1:100) and Gli2 (ABCam Inc., dilution of 1:1,000). Positive staining is shown in brown (indicated by arrows in stroma and arrowheads in the tumor). Hematoxylin was used for counter staining (blue in the nucleus). Phospho-SMAD2/3 staining was shown in tumor as well as in the stroma whereas Gli2 staining was positive mainly in the stroma.

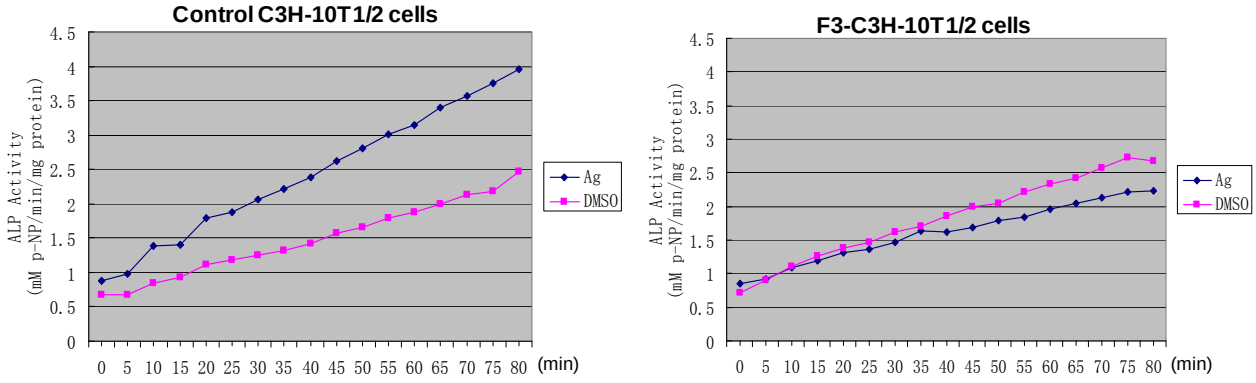

Fig. S4- Measurement of alkaline phosphatase level by spectrophotometry using the Sensolyte pNPP Alkaline Phosphatase Assay kit (AnaSpec, San Jose, CA, http:// www.anaspec.com) Cells were incubated with the substrate for 80 min and the optical density was measured every 5 min. In the control cells, Smo agonist purmorphamine (indicated as Ag at the left) treatment led to a significant increase of ALP activity in comparison with DMSO treatment. In contrast, TGFβ2 knocking down prevented purmorphamine-induced ALP activity increase (right figure, no significant differences between Ag-treated and DMSO-treated).

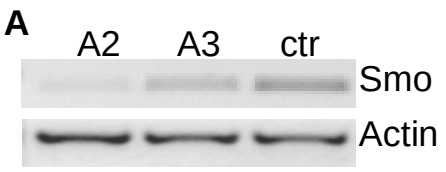

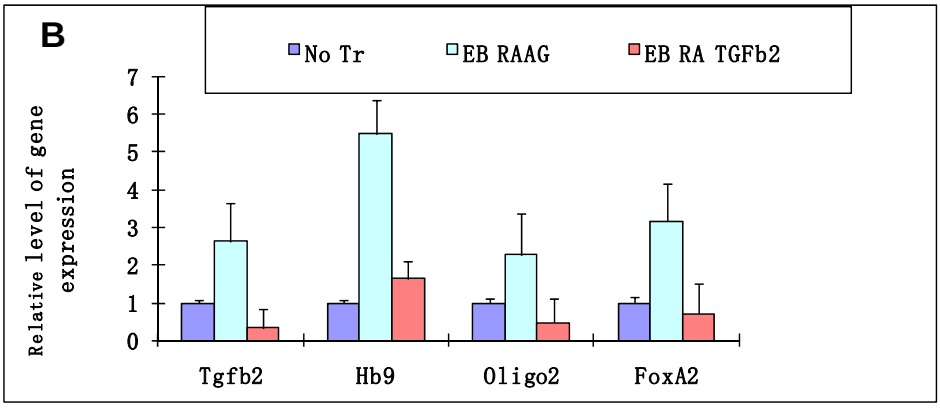

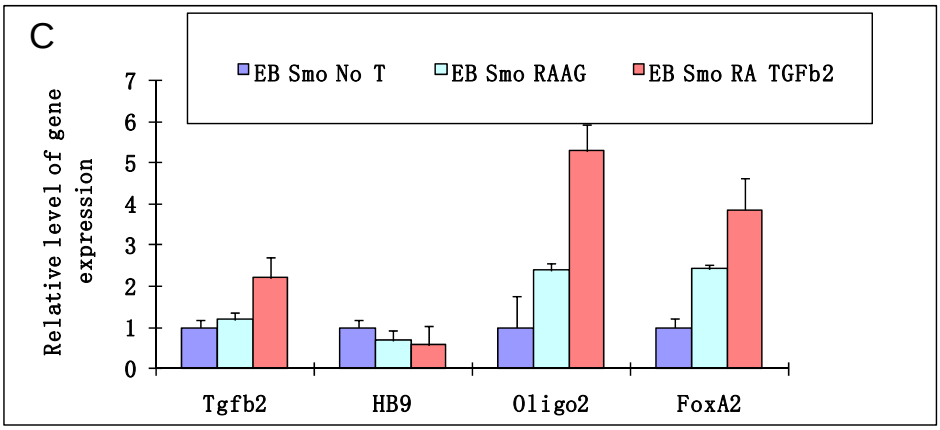

Fig. S5. The effect of TGFβ2 for motor neuron differentiation in the absence of Smo. **A.** Smo gene expression was knocked down by shRNAs, and examined by RT-PCR. Clone A2 gave the highest silencing of Smo. **B.** Real-time PCR analysis of TGFβ2 and motor neuron markers after treatment with retinoid acid (indicated as RA) and purmorphamine (indicated as AG) or TGFβ2. Whereas AG induced motor neuron marker expression, TGFβ2 did not **C**. After knocking down Smo, most markers were not induced. We noticed that TGFβ2 induced expression of early markers oligo2 and FoxA2, indicating that although TGFβ2 is required for Smo-mediated motor neuron differentiation, it is not sufficient to drive this process.

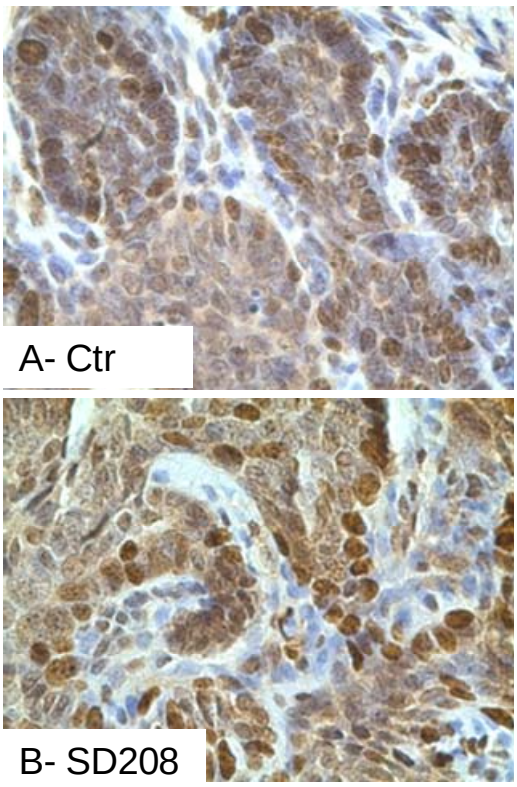

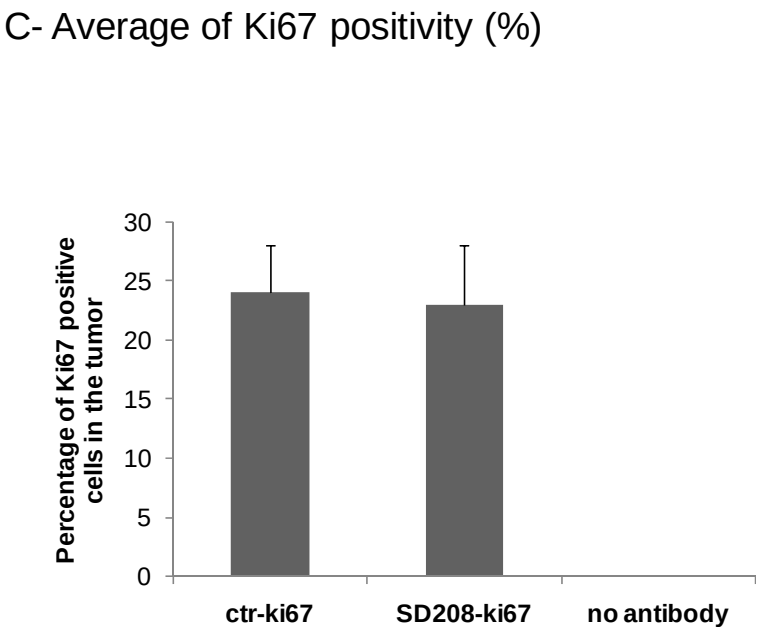

Fig. S6 Detection of Ki67 in mouse skin tumors. Immunohistochemistry was performed as described in **Fig. S2**. Ki67 antibodies (ABCam) was diluted 1:400. Positive staining is in brown in the nucleus. Hematoxylin was used for counter staining (blue). An average of Ki67 positivity from 8 different areas was calculated and represented in **C**.

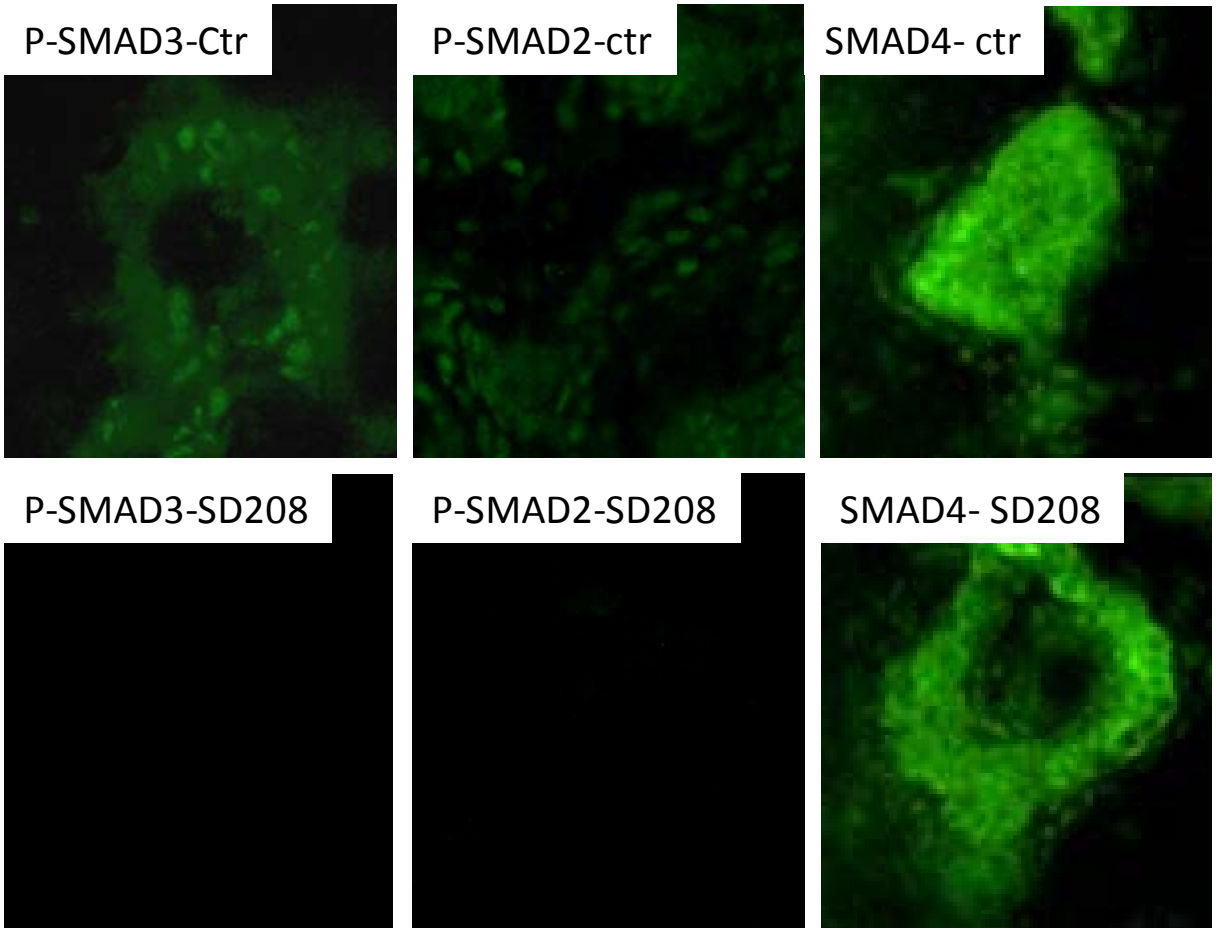

Fig. S7 Regulation of the phosphorylated SMAD2, SMAD3 and total SMAD4 levels by SD208. To examine the specificity of TGFbRI kinase inhibitor SD208 in mouse skin with BCCs, we detected the levels of phosph-SMAD2/3 as well as total SMAD4 in mouse skin specimens treated with SD208 or the control solvent. Using immunofluorescent staining and antibodies specific to SMADs (phosph-SMAD2 and SMAD4 from Cell Signaling Inc., 1:200 dilution; phosph-SMAD3 from Santa Cruz Biotech Inc., 1:200), phosph-SMAD2 and SMAD3 can be detected in mouse tumors without SD208 treatment. However, they were undetectable following SD208 treatment. As a control, the total level of SMAD4 (antibodies from Cell Signaling Inc., with 1:100 dilution) was not much changed by SD208 treatment, but more cytoplasmic location was seen in SD208 treated tissue. Similarly, total SMAD2 and SMAD3 was not changed by SD208 (data not shown).

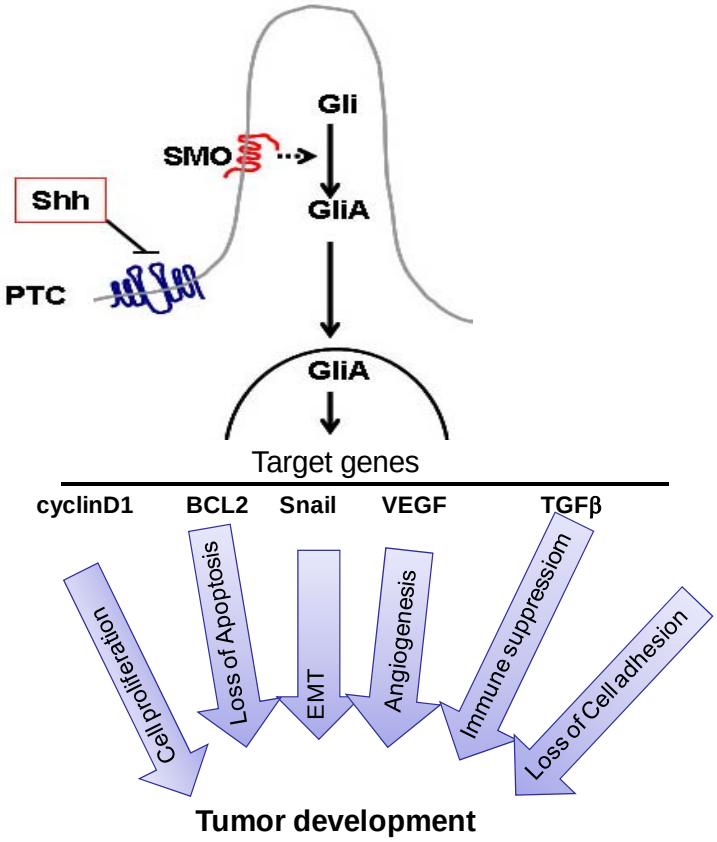

Fig. S8. A proposed diagram for Hh signaling-signaling and BCC development. Development of BCCs is associated with several cellular changes. However, the underlying molecular mechanisms for these cellular processes are not entirely clear. Based on previously published papers and our studies in the manuscript, we propose a model that Hh target genes are responsible for some of these processes. Hh target gene Cyclin D1 is known to regulate cell proliferation. Bcl2, another Hh target gene, is known to inhibit apoptosis. VEGF and IGF-2 are known Hh regulating genes associated with angiogenesis. Although Epithelial-mesenchymal transition (EMT) is not dramatic in BCCs, loss of keratin expression is common. Snail is a Hh regulating gene. Our data indicate that TGFβ signaling mediates immune suppression in SmoM2-induced skin tumors. Although each target gene may have more than one function, we believe that it takes more than one target genes to reproduce the Hh signaling-mediated effects.